JM RAPIDS

Subcritical transition to turbulence in quasi-two-dimensional shear flows

Christopher J. Camobreco[1,2]**, Alban Pothérat**[3,†] **and Gregory J. Sheard**[1]

[1]Department of Mechanical and Aerospace Engineering, Monash University, Victoria 3800, Australia

[2]Department of Mechanical Engineering, University of Melbourne, Victoria 3010, Australia

[3]Fluid and Complex Systems Research Centre, Coventry University, Coventry CV15FB, UK

The transition to turbulence in conduits is among the longest-standing problems in fluid mechanics. Challenges in producing or saving energy hinge on understanding promotion or suppression of turbulence. While a global picture based on an intrinsically 3-D subcritical mechanism is emerging for 3-D turbulence, subcritical turbulence is yet to even be observed when flows approach two dimensions, e.g. under intense rotation or magnetic fields. Here, stability analysis and direct numerical simulations demonstrate a subcritical quasi-two-dimensional (quasi-2-D) transition from laminar flow to turbulence, via a radically different 2-D mechanism to the 3-D case, driven by nonlinear Tollmien–Schlichting waves. This alternative scenario calls for a new line of thought on the transition to turbulence and should inspire new strategies to control transition in rotating devices and nuclear fusion reactor blankets.

1. Introduction

One of the most important questions in fluid mechanics is how, and under what conditions, flows transition to a turbulent state; this determines the topological, dissipative and mixing properties of these flows. Besides its fundamental interest as a unique physical process, it is central to every application where fluid flows through a conduit: turbulent mixing promotes heat exchange in cooling applications, whereas turbulent dissipation drastically increases energy consumption. As discovered by Reynolds (1883), the flow of water through a pipe became turbulent only for sufficiently high values of the eponymous Reynolds number $Re = U_0 L/\nu$. In the present work, Re is built out of the typical

streamwise velocity U_0 and kinematic viscosity ν of the fluid, and the transverse conduit length scale $2L$. Since then, the question of transition was often tackled by seeking the conditions necessary for perturbations growing from the laminar base flow to ignite turbulence.

In pipes and other shear flows, the most distinctive property of the transition to turbulence is that it is subcritical. If Re_c is the critical Reynolds number beyond which some perturbation grows exponentially from an infinitely small amplitude through a linear mechanism, turbulence can develop at $Re < Re_c$, provided the flow is seeded with a sufficiently energised perturbation. The process is nonlinear and amplifies finite amplitude perturbations through an intrinsically 3-D 'lift-up' mechanism, enacted by the growth of streamwise streaks (Schmid & Henningson 2001). It also becomes active at Reynolds numbers well below Re_c, where infinitesimal perturbations are severely damped. For convenience we define $r_c = Re/Re_c$, where subcritical Reynolds numbers correspond to $r_c < 1$. The least damped perturbations are the 2-D transverse-invariant Tollmien–Schlichting waves (TS waves), which manifest in plane shear flows. For instance, Beneitez *et al.* (2019) showed that TS waves were not found to partake in the 3-D transition to turbulence below $r_c \simeq 0.98$ in Blasius boundary layers, while Zammert & Eckhardt (2019) showed that they could not be detected in plane Poiseuille flow for $r_c \lesssim 0.84$.

However, in rapidly rotating or stratified flows, or in an electrically conducting fluid subjected to a high magnetic field, fluid motion can be prevented from becoming 3-D if the respective Coriolis, buoyancy or Lorentz forces are sufficiently intense. Hydraulic circuits in rotating machines, atmospheres, oceans and some models of planetary interiors subject to planetary rotation, and the liquid metal blankets cooling fusion reactors, all occupy this category. Real flows can never be fully 2-D (Paret *et al.* 1997; Akkermans *et al.* 2008); three-dimensionality subsists either in asymptotically small measure or in asymptotically small regions such as boundary layers (Sansón & van Heijst 2000; Pothérat 2012). The resulting flows are quasi-two-dimensional (quasi-2-D). Since the lift-up mechanism driving transition in 3-D shear flows cannot manifest in quasi-2-D flows, can subcritical quasi-2-D turbulence exist, and if so via which alternative transition mechanism?

Traditionally, quasi-2-D turbulence has 'only' been considered as a limit-state of its 3-D counterpart (Moffatt 1967; Sommeria & Moreau 1982; Shats, Byrne & Xia 2010), perhaps because both very often coexist (Celani, Musacchio & Vincenzi 2010). For example, atmospheric flows are quasi-2-D at large, continental scales, but 3-D nearer to topographic scales (Lindborg 1999). A similar spectral split exists in magnetohydrodynamic turbulence (Baker *et al.* 2018) and in turbulence in thin channels (Benavides & Alexakis 2017). Quasi-2-D turbulence appears progressively rather than through a bifurcation, and is controlled by the constraint driving two-dimensionality (Sommeria & Moreau 1982; Pothérat & Klein 2014; Benavides & Alexakis 2017). Turbulent transition in quasi-2-D shear flows differs from the switch between 3-D and 2-D turbulence as it is expected to arise suddenly, out of (quasi-)2-D finite amplitude instabilities. Since 3-D mechanisms are excluded, the question is whether there exists a quasi-2-D subcritical transition pathway from the laminar to the turbulent state. This is particularly crucial in shear flows as the subcritical lift-up transition is progressively suppressed as two-dimensionality is established (Cassells *et al.* 2019). The key result presented in this paper is the discovery of a transition from the quasi-2-D laminar state to subcritical quasi-2-D turbulence in shear flows, and that the lack of a 3-D bypass mechanism gives way to an alternative nonlinear 2-D mechanism which, unlike its 3-D counterpart, relies on TS waves.

2. Physical model

All calculations are performed on a rectangular incompressible duct flow, with walls in the (x, z) plane moving at a constant velocity $U_0 e_x$ ($e_{x,y,z}$ are unit vectors in the respective x, y, z directions). The base flow is streamwise invariant and periodic boundary conditions are imposed in the streamwise direction (x). The flow is assumed quasi-2-D, i.e. all quantities are invariant in z except in thin boundary layers near the fixed walls in (x, y) planes (see figure 1). Such flows are well described by the 2-D, z-averaged Navier–Stokes equations for z-averaged velocity and pressure supplemented by a linear friction term accounting for the friction these layers impart. With length, velocity, time and pressure respectively scaled by L, U_0, L/U_0 and ρU_0^2, these equations are

$$\nabla_\perp \cdot \boldsymbol{u}_\perp = 0, \quad \partial_t \boldsymbol{u}_\perp + (\boldsymbol{u}_\perp \cdot \nabla_\perp)\,\boldsymbol{u}_\perp = -\nabla_\perp p_\perp + Re^{-1}\left(\nabla_\perp^2 \boldsymbol{u}_\perp - H\boldsymbol{u}_\perp\right), \quad (2.1)$$

with dimensionless boundary conditions $\boldsymbol{u}_\perp(y = \pm 1) = (1, 0)$, where $\boldsymbol{u}_\perp = (u_\perp, v_\perp)$, $\nabla_\perp = (\partial_x, \partial_y)$, $\nabla_\perp^2 = \partial_x^2 + \partial_y^2$, ρ is the fluid density, and $2L$ the distance between the moving walls. Friction parameter H may be defined as appropriate to describe systems including duct flows under a strong transverse magnetic field Be_z (Sommeria & Moreau 1982), thin films (Bühler 1996), or flows with background rotation (with the addition of the Coriolis force) (Pedlosky 1987).

We investigate perturbations $\hat{\boldsymbol{u}}_\perp$ about the base flow $U_\perp(y) = (\cosh[H^{1/2}y]/\cosh[H^{1/2}], 0)$ at $H = 10$. Here linear perturbations become unstable at $Re_c = 79\,123.2$. At $r_c = 0.9$, the maximum linear transient growth occurs at a streamwise wavenumber $\alpha_{opt} = 1.49$, whereas the minimum exponential decay occurs at $\alpha_{max} = 0.979651$. The linearly optimised initial perturbation maximising growth in the functional $G = \|\hat{\boldsymbol{u}}_\perp(t = \tau)\|/\|\hat{\boldsymbol{u}}_\perp(t = 0)\|$ is sought following Barkley, Blackburn & Sherwin (2008) for a prescribed target time τ and wavenumber α. Here G represents the gain in perturbation kinetic energy under the norm $\|\hat{\boldsymbol{u}}_\perp\| = \int \hat{\boldsymbol{u}}_\perp \cdot \hat{\boldsymbol{u}}_\perp \, d\Omega$, over computational domain Ω. Optimisation is performed on the linearised rather than the full nonlinear equation, though both return practically identical results for this problem (Camobreco, Pothérat & Sheard 2020). The choice of α is based on the decay rate of the leading direct eigenmode, obtained by decomposing perturbations into normal modes $(\tilde{\boldsymbol{u}}_\perp, \tilde{p}_\perp) \exp(i[\alpha x - \omega t])$ of complex frequency ω, and complex velocity and pressure distributions $\tilde{\boldsymbol{u}}_\perp$ and $\tilde{p}_\perp$. A discretised direct eigenvalue problem $-i\omega \tilde{v}_\perp = L\tilde{v}_\perp$ is solved in MATLAB via eigs(iL). The linear evolution operator L is constructed following Trefethen *et al.* (1993) and Schmid & Henningson (2001). The discretised adjoint eigenvalue problem $i\omega^\ddagger \tilde{\xi}_\perp = L^\ddagger \tilde{\xi}_\perp$ for complex adjoint eigenvector $^\ddagger\tilde{\xi}_\perp$ is also considered, where the linear adjoint operator $L^\ddagger$ is derived following Schmid & Henningson (2001).

To support the classification of initial conditions realising turbulence, streamwise Fourier spectra of kinetic energy are computed at selected instants in time at 21 equi-spaced y-values spanning the channel. At each y-location, a Fourier transform is obtained along x, with coefficients for the streamwise wavevector κ, $c_\kappa(y) = N_f^{-1} \sum_{n=0}^{N_f-1} |\hat{\boldsymbol{u}}_\perp(x_n, y)|^2 \exp(-2\pi i \kappa n/N_f)$, where the nth coefficient $x_n = 2\pi n/(\alpha N_f)$ spans the streamwise-periodic domain. Here for convenience the coefficient N_f^{-1} is applied to the forward transform rather than its inverse. Instantaneous mean Fourier coefficients $\bar{c}_\kappa$ are then obtained by averaging $|c_\kappa|$ over y.

Time evolution of the full quasi-2-D equations or the linear forward and adjoint systems is computed numerically using a primitive variable spectral element solver (Hussam, Thompson & Sheard 2012; Cassells *et al.* 2019; Camobreco *et al.* 2020; Camobreco, Pothérat & Sheard 2021b). The (x, y) plane is discretised with quadrilateral elements
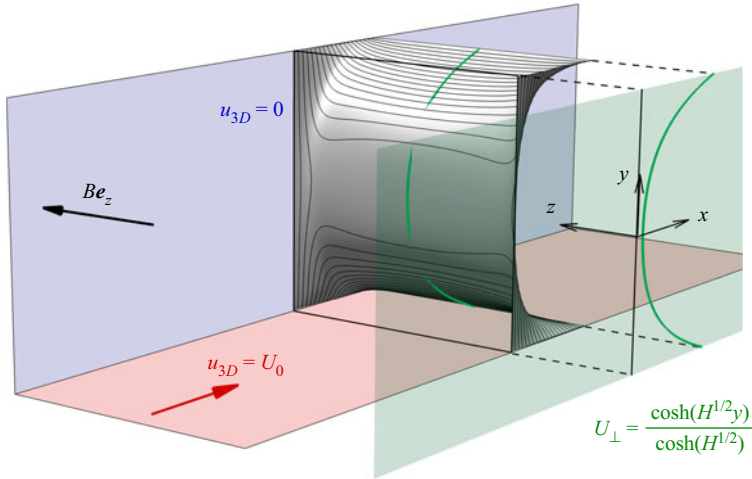
Figure 1. An example of a quasi-2-D flow is shown, namely a lateral wall-driven laminar duct flow under a transverse magnetic field. Here the solution (green profile, $H = 10$) obtained from the quasi-2-D equations (2.1) precisely approximates the z-average of the 3-D streamwise velocity profile u_{3D} (grey isosurface, black contour lines) satisfying the quasi-static magnetohydrodynamic equations (Müller & Bühler 2001). Beyond this example, the results derived in this paper apply to a much wider variety of flows.

(12 by 48) featuring polynomial basis functions of order $N_p = 19$ (Camobreco *et al.* 2020, 2021*b*; Camobreco, Pothérat & Sheard 2021*a*). Time integration is via third-order backward differencing, with operator splitting (Karniadakis, Israeli & Orszag 1991). The time step size is initially set to $\Delta t = 1.25 \times 10^{-3}$, and is reduced once turbulence emerges to maintain stability. The initial condition is composed of the laminar base flow and a perturbation computed via linear transient growth optimisation. The domain length is matched to the wavelength minimising the decay rate of the leading eigenmode. The perturbation amplitude is normalised to the energy E_0 required for each simulation.

3. Evidence of subcritical turbulence

The starting point is to determine whether subcritical turbulence in quasi-2-D shear flows exists (for $Re < Re_c$). In the subcritical regime, turbulence originates from perturbations that are sufficiently intense to activate nonlinear amplification mechanisms that infinitesimal ones cannot. Unlike 3-D flows, there is evidence that seeding the subcritical laminar shear flow with even high levels of noise does not ignite turbulence (Camobreco *et al.* 2021*b*). Seeking turbulence, but not necessarily its most efficient trigger, the laminar state is seeded with optimal transient growth perturbations of different energies, and evolved until the flow either returns to its initial laminar state or becomes turbulent.

Figure 2(*a*) depicts a representative set of the aforementioned simulations at a Reynolds number $r_c = 0.9$. A turbulent state is reached for any normalised initial energy $E_0 > E_D$, where $E_0 = E/E_B$. Here E is the kinetic energy of the disturbance, and E_B is the energy of the laminar base flow. The delineation energy E_D, found when seeding the flow with optimal perturbations from linear transient growth analysis, lies within $3.0576 \times 10^{-6} < E_D < 3.0577 \times 10^{-6}$. Evidence of a turbulent state is found in the energy spectra $\bar{c}_\kappa(\kappa)$ of figure 2(*b*): while low energy states contain energy above the noise floor (around 10^{-13}) in only a few of the lower wavenumber modes, all modes are energised in the turbulent cases (Grossmann 2000), with an extended inertial range following $\bar{c}_\kappa(\kappa) \sim \kappa^{-5/3}$ (Tabeling
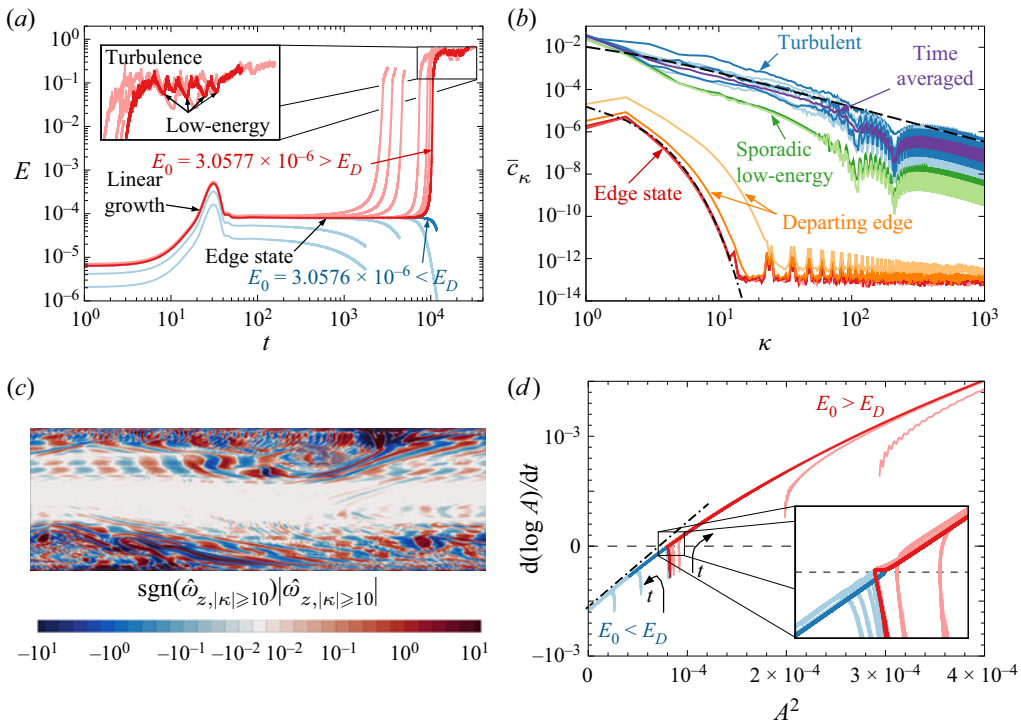
Figure 2. (*a*) Kinetic energy time history showing the nonlinear evolution of linear optimals at $r_c = 0.9$, α_{max}: when $E_0 < E_D$ (blue) the flow visits the edge but relaminarises, whereas it becomes turbulent for $E_0 > E_D$ (red). (*b*) Fourier spectra at select instants in time at $E_0 = 3.0577 \times 10^{-6} > E_D$. Dash-dotted line, $\exp(-3\kappa/2)$ trend. Dashed line, $\kappa^{-5/3}$ trend. (*c*) Streamwise high-pass filtered snapshot of spanwise vorticity $|\hat{\omega}_{z,|\kappa|\geq 10}|$ from DNS at $r_c = 0.9$, α_{max}, indicating quasi-2-D turbulence at $t = 1.1 \times 10^4$. (*d*) Data from (*a*) re-plotted under the framework of the Stuart–Landau model. The instantaneous growth rate of the perturbation amplitude A is plotted against A^2. The data exhibits a collapse onto a common curve exhibiting the signature of a subcritical bifurcation, i.e. approaching the eigenmode growth rate $\mathrm{Im}(\omega) = -5.94084 \times 10^{-4}$ as $A \to 0^+$ with a positive gradient. For guidance, the dot-dashed line is tangent to this curve at $A = 0$.

2002). These features are characteristic of turbulence, a snapshot of which is visualised in figure 2(*c*). This visualisation employs a streamwise high-pass filter to remove the otherwise occluding large-scale TS wave structures. This filter reveals smaller-scale structures being entrained from the sidewall boundary layers into the channel interior. Instances of this are visible near the bottom wall at the upstream end of the domain, and further downstream near the top wall. The respective locations of these features align with the entrainment regions of the underlying TS wave.

With the existence of subcritical turbulence in quasi-2-D flows now established, two remarkable features emerge. First, the turbulence is intermittent in time, exhibiting sporadic regressions to a low energy state differing from the original laminar state (figure 2*a*). This is reminiscent of the spatial intermittency in various 3-D shear flows (Cros & Gal 2002; Barkley & Tuckerman 2007; Moxey & Barkley 2010; Brethouwer, Duguet & Schlatter 2012; Khapko *et al.* 2014). Second, transition to indefinitely sustained turbulence was only found for $Re \gtrsim 0.8 Re_c$. Hence the Reynolds numbers required to sustain turbulence are much higher than in 3-D flows. Over $0.4 \lesssim r_c \lesssim 0.8$, only a single turbulent episode was observed, with finite lifetime proportional to Re.

Verification that the turbulence reported herein originates from a subcritical instability is determined using the Stuart–Landau model (Drazin & Reid 2004) following the approach detailed in Sapardi *et al.* (2017), a brief outline of which is explained here. The time history of a measure of the disturbance amplitude $A(t) = \sqrt{\int_\Omega |\hat{u}_\perp|^2 \, d\Omega}$ is taken, with subcritical bifurcation evolution characterised by an increase in $d(\log A)/dt$ with increasing amplitude near $A = 0$. Beyond the critical Reynolds number, an infinitesimal disturbance achieves super-exponential growth before saturating. Below the critical Reynolds number, small disturbances decay, while larger-amplitude disturbances grow. This behaviour is observed in figure 2(*d*). Cases bracketing E_D approach a common curve having the expected subcritical profile; cases with $E < E_D$ then decay ($d(\log A)/dt < 0$, $A \to 0$), while $E > E_D$ cases grow towards turbulence.

4. Nonlinear Tollmien–Schlichting waves are the tipping point between laminar and turbulent states

Having established that subcritical turbulence exists, we consider the pathway from the laminar base flow to the turbulent state. We now seek edge states. These act as tipping points from which the flow can either revert to its original laminar state, or become turbulent (Skufca, Yorke & Eckhardt 2006). The edge state is reached for the initial perturbation delineation energy E_D, separating perturbations triggering turbulence from those decaying. As the initial energy approaches E_D, the edge state persists for a longer duration. Here E_D is found iteratively with a bisection method (Itano & Toh 2001). The edge state from figure 2(*a*) is visualised in figure 3(*a*). It consists of a travelling wave of very similar topology to the infinitesimal TS wave, suggesting they may play a role in the quasi-2-D transition to turbulence.

To investigate this possibility, we calculated a weakly nonlinear flow state in which nonlinearities only arise out of combinations of the leading TS wave. The weakly nonlinear equations are a more precise version of the perturbation equations compared with the linearised version used to calculate the leading eigenmode and the perturbation maximising transient growth. They are obtained by approximating the perturbation by the leading eigenmode, and truncating its governing equations to the third order in its amplitude. For example, for a leading eigenmode of amplitude ϵ, the nth harmonic of the spanwise velocity component is written as

$$\hat{v}_{\perp,n} = \sum_{m=0}^{\infty} \epsilon^{|n|+2m} \tilde{A}^{|n|} |\tilde{A}|^{2m} \hat{v}_{\perp,n,|n|+2m}, \tag{4.1}$$

where $\hat{v}_{\perp,n,|n|+2m}$ denotes a perturbation (n refers to the harmonic, $|n| + 2m$ to the amplitude order) and $\tilde{A} = A/\epsilon$ is the normalised amplitude. Nonlinear self-interaction of the linear mode $\hat{v}_{\perp,1,1}$ excites a second harmonic $\hat{v}_{\perp,2,2}$, which is compared to the $\kappa = 2$ harmonic from DNS. Nonlinear interaction between the linear mode $\hat{v}_{\perp,1,1}$ and its complex conjugate $\hat{v}_{\perp,-1,1}$ generates a modification to the base flow $\hat{u}_{\perp,0,2}$, which is compared to the $\kappa = 0$ harmonic from DNS. The full equations governing the nth harmonic of the base flow and perturbation follow from insertion of this decomposition into (2.1); they are expressed in full in Camobreco *et al.* (2021*b*) and the general method is detailed in Hagan & Priede (2013). The full nonlinear evolution of the flow is obtained by solving the system (2.1) numerically.

This technique facilitates a comparison between the fully nonlinear flow state (with all possible modes) obtained from DNS, with its asymptotic approximation to second order
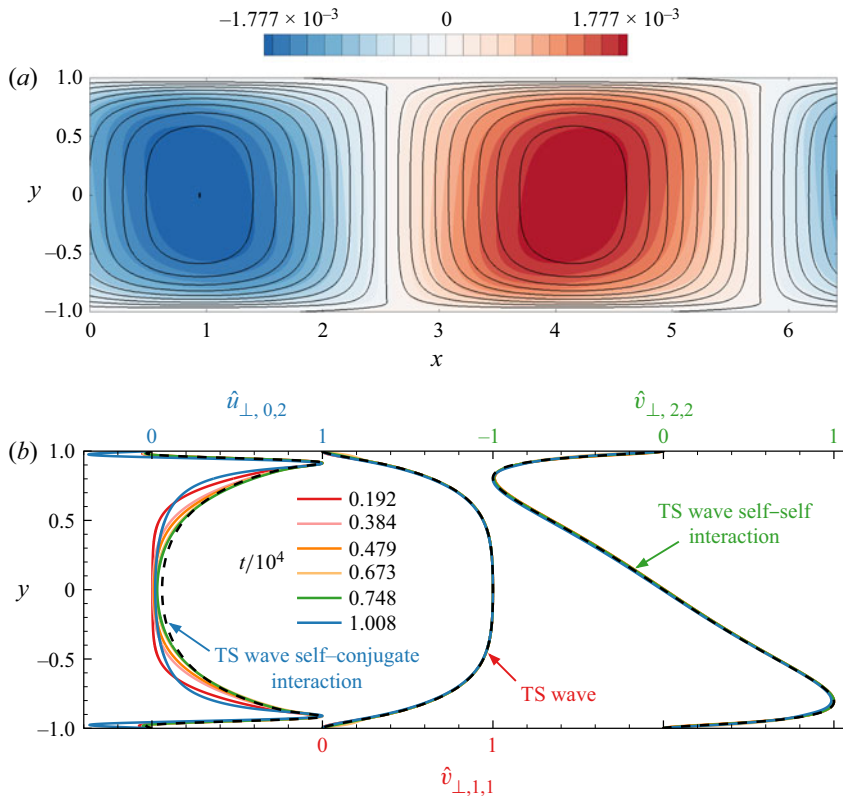
Figure 3. (*a*) Flooded contours of spanwise velocity $\hat{v}_\perp$ from DNS at $r_c = 0.9$, α_{max}, representing the edge state at $t = 7.48 \times 10^3$ overlaid with contour lines showing the linear TS wave $\hat{v}_{\perp,1,1}$. Both sets of contours are equi-spaced between the minimum and maximum values of the respective fields. (*b*) Weakly nonlinear modes $\hat{u}_{\perp,0,2}$, $\hat{v}_{\perp,1,1}$, $\hat{v}_{\perp,2,2}$ (dashed black lines) and corresponding Fourier components from DNS at different times (coloured lines) at $\kappa = 0$ (streamwise), 1 (spanwise) and 2 (spanwise) with $E_0 = 3.0577 \times 10^{-6} > E_D$. The solution departs the edge at $t \approx 9 \times 10^3$.

in the perturbation amplitude. The streamwise $\kappa = 1$ Fourier mode extracted from DNS is directly compared to the linearly computed modal instability in figure 3(*a*), showing close agreement.

Figure 3(*b*) compares velocity profiles from each of the modes accounted for in the weakly nonlinear analysis with the corresponding Fourier components of the same wavelength extracted from the full DNS evolved from the linear optimal with $\alpha = \alpha_{max}$ with E_0 close to E_D. Both the leading eigenmode ($\kappa = 1$) and its nonlinear interaction ($\kappa = 2$) matched their DNS counterpart to high precision in the early stage of evolution. The modulated streamwise-independent ($\kappa = 0$) component exhibited small differences at this stage, that vanished as the influence of our particular choice of initial condition did. Additionally, the cumulated kinetic energy of all three components forming the weakly nonlinear approximation represents over 93.7 % of the total energy in the DNS while on the edge. This proves that the build-up of the edge state originates almost exclusively from the dynamics of the TS wave. As such, this transition mechanism differs radically from its counterpart in 3-D flows (Zammert & Eckhardt 2019), where a bypass transition involving rapidly growing streamwise structures takes place at such low Reynolds numbers that TS waves are too damped to contribute.
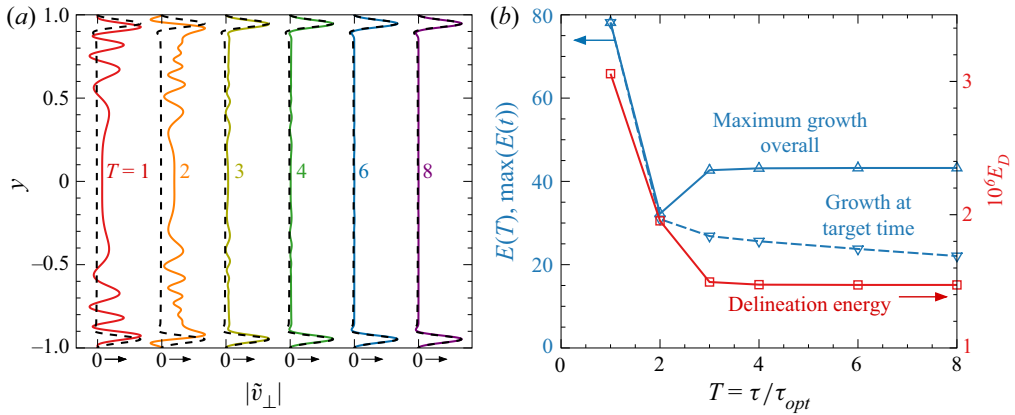
Figure 4. (*a*) Comparison between linear transient growth initial conditions with various $\tau = T\tau_{opt}$ (solid lines) and the leading adjoint mode (dashed lines), horizontally shifted for clarity. (*b*) Delineation energies from DNS and energy growth ratios from linear analysis for each T.

With the pathway to the edge state and then to turbulence now clarified, the question remains as to its robustness against the choice of initial condition. Thus, DNS were performed with the initial conditions chosen as the modes optimising growth at increasingly large times $T = \tau/\tau_{opt}$ (where τ_{opt} is the time of optimal growth for a given wavenumber α, i.e. $\tau_{opt} \simeq 31.0$ for $\alpha = \alpha_{max}$ at $r_c = 0.9$). The corresponding delineation energy provides a measure of how easily these transients ignite turbulence and therefore of their role in doing so.

In these simulations, all optimals for a given α evolved into the same edge state. Further, as T increases, the profiles of spanwise velocity of the initial condition optimising growth with $\alpha = \alpha_{max}$ converge toward the leading adjoint mode (figure 4*a*), with a corresponding monotonic reduction in the delineation energy with increasing T (figure 4*b*). By $T = 8$, the delineation energy of the optimal matches that of the leading adjoint to approximately $\pm 0.01\,\%$. Figure 4(*b*) further shows that these initial conditions lead to reduced transient growth, yet are more efficient at triggering turbulence: that is to say, the delineation energy E_D decreased approximately twofold as the initial condition morphed from the linear optimal mode to the linear adjoint mode. This was found to be consistent when the streamwise wavenumber was varied. Duguet, Brandt & Larsson (2010) similarly showed that maximising transient growth does not necessarily imply an easier transition. Hence the leading adjoint eigenmode, which by construction optimally energises the TS wave, is a more efficient initial condition to reach turbulence than any initial condition producing optimal transient growth. Consequently, optimal growth does not favour the transition, unlike in 3-D shear flows where the transient growth associated with the lift-up mechanism is an essential element of the transition process (Reddy *et al.* 1998; Pringle, Willis & Kerswell 2012).

The same procedures applied at lower r_c produced the same reduction in delineation energy with increasing T and exhibited edge states independent of T. For $0.3 \lesssim r_c \lesssim 0.8$, after departing the edge, a secondary stable state formed (Jiménez 1990; Falkovich & Vladimirova 2018), again independent of the initial condition.

5. Discussion and concluding remarks

In conclusion, subcritical turbulence exists in quasi-2-D shear flows and can be reached directly, rather than via an intermediate 3-D state. The 2-D transition mechanism bears

963 R3-8

important similarities with its 3-D cousin: it is ignited by a perturbation of finite amplitude and first reaches an edge state that is seemingly independent of this initial perturbation. The edge state subsequently breaks down into a turbulent state if the initial perturbation energy exceeds the delineation energy E_D for that particular perturbation. As in the 3-D problem, the attained turbulence is not yet fully developed (Wygnanski & Champagne 1973; Wygnanski, Sokolov & Friedman 1975). Departure from fully established turbulence in quasi-2-D shear flows expresses as time intermittency, with sporadic retreats to a low energy state different from the base laminar flow.

Conversely, the subcritical transition in quasi-2-D shear flows exhibits specificities that distinguish it sharply from the 3-D one. Chiefly, the lift-up mechanism that underpins transitions in 3-D can be ignited at criticality so low that the TS waves are strongly suppressed by the linear dynamics, despite being the least damped infinitesimal perturbation. Thus, they are not observed in the 3-D transition. In quasi-2-D flows by contrast, the 3-D mechanism is absent and our study demonstrates that the dynamics is dominated by the TS waves, with the edge state resulting directly from their weakly nonlinear evolution. In a quasi-2-D flow, the TS wave instability directly connects the base flow to turbulence via a subcritical bifurcation, in stark contrast to a 3-D flow in which the saddle-node bifurcation is disconnected from the base state (Khapko *et al.* 2014). This may also explain why transition in quasi-2-D flows is relatively weakly subcritical: at lower r_c, TS waves are so strongly linearly damped that their nonlinear growth is stifled.

This new transition mechanism reopens many questions resolved in the 3-D case: How does the intermittency or localisation of the turbulence evolve into the supercritical regime, e.g. following the mechanism outlined by Mellibovsky & Meseguer (2015)? Does the transition to the fully turbulent state obey a second-order phase transition of the universality class of directed percolations as for other shear flows (Lemoult *et al.* 2016)? While the thermodynamic formalism used by Wang, Li & Weinan (2015) indicates that two-dimensional Poiseuille flow loses stability in a manner consistent with a continuous phase transition, in the quasi-2-D case linear friction may impact the development and interaction of unstable travelling waves, and so this remains an open question. Separately, much remains to be discovered on the subcritical response to finite amplitude perturbations: How does the delineation energy vary with criticality, especially considering the relatively short subcritical range in which turbulence can be sustained? Can this subcritical response be manipulated to prevent or promote turbulence (for example, to enhance heat transfer in the heat exchangers of plasma fusion reactors)? These questions call for expensive numerical simulations, but also for experiments with well-controlled perturbations, since this first evidence of subcritical transitions in quasi-2-D shear flows is currently purely numerical.

While we have established a scenario for transition involving a purely 2-D mechanism, 3-D mechanisms could still compete with this scenario and trigger a subcritical 3-D transition. Whether one of the other scenarios dominates cannot be determined on the basis of (2.1) only as the 3-D mechanisms are specific to the physical process promoting the emergence of quasi-2-D dynamics. As such, whether a purely quasi-2-D subcritical transition to turbulence can be observed in practice remains to be determined in particular cases. The question could be addressed either with 3-D numerical methods or experiments on magnetohydrodynamics or rotating flows, or in Hele-Shaw cells, for example.

Author ORCIDs.

Ⓘ Christopher J. Camobreco https://orcid.org/0000-0001-7068-3204;

Ⓘ Alban Pothérat https://orcid.org/0000-0001-8691-5241;

Ⓘ Gregory J. Sheard https://orcid.org/0000-0003-0836-1524.

REFERENCES

AKKERMANS, R.A.D., KAMP, L.P.J., CLERCX, H.J.H. & VAN HEIJST, G.J.F. 2008 Intrinsic three-dimensionality in electromagnetically driven shallow flows. *Europhys. Lett.* **83** (2), 24001.

BAKER, N.T., POTHÉRAT, A., DAVOUST, L. & DEBRAY, F. 2018 Inverse and direct energy cascades in three-dimensional magnetohydrodynamic turbulence at low magnetic Reynolds number. *Phys. Rev. Lett.* **120**, 224502.

BARKLEY, D., BLACKBURN, H.M. & SHERWIN, S.J. 2008 Direct optimal growth analysis for timesteppers. *Intl J. Numer. Meth. Fluids* **57**, 1435–1458.

BARKLEY, D. & TUCKERMAN, L.S. 2007 Mean flow of turbulent-laminar patters in plane Couette flow. *J. Fluid Mech.* **576**, 109–137.

BENAVIDES, S.J. & ALEXAKIS, A. 2017 Critical transitions in thin layer turbulence. *J. Fluid Mech.* **822**, 364–385.

BENEITEZ, M., DUGUET, Y., SCHLATTER, P. & HENNINGSON, D.S. 2019 Edge tracking in spatially developing boundary layer flows. *J. Fluid Mech.* **881**, 164–181.

BRETHOUWER, G., DUGUET, Y. & SCHLATTER, P. 2012 Turbulent-laminar coexistence in wall flows with Coriolis, buoyancy or Lorentz forces. *J. Fluid Mech.* **704**, 137–172.

BÜHLER, L. 1996 Instabilities in quasi-two-dimensional magnetohydrodynamic flows. *J. Fluid Mech.* **326**, 125–150.

CAMOBRECO, C.J., POTHÉRAT, A. & SHEARD, G.J. 2020 Subcritical route to turbulence via the Orr mechanism in a quasi-two-dimensional boundary layer. *Phys. Rev. Fluids* **5** (11), 113902.

CAMOBRECO, C.J., POTHÉRAT, A. & SHEARD, G.J. 2021*a* Stability of pulsatile quasi-two-dimensional duct flows under a transverse magnetic field. *Phys. Rev. Fluids* **6** (5), 053903.

CAMOBRECO, C.J., POTHÉRAT, A. & SHEARD, G.J. 2021*b* Transition to turbulence in quasi-two-dimensional MHD flow driven by lateral walls. *Phys. Rev. Fluids* **6** (1), 013901.

CASSELLS, O.G.W., VO, T., POTHÉRAT, A. & SHEARD, G.J. 2019 From three-dimensional to quasi-two-dimensional: transient growth in magnetohydrodynamic duct flows. *J. Fluid Mech.* **861**, 382–406.

CELANI, A., MUSACCHIO, S. & VINCENZI, D. 2010 Turbulence in more than two and less than three dimensions. *Phys. Rev. Lett.* **104** (18), 184506.

CROS, A. & GAL, P.L. 2002 Spatiotemporal intermittency in the torsional Couette flow between a rotating and a stationary disk. *Phys. Fluids* **14** (11), 3755–3765.

DRAZIN, P.G. & REID, W.H. 2004 *Hydrodynamic Stability*. Cambridge University Press.

DUGUET, Y., BRANDT, L. & LARSSON, B.R.J. 2010 Towards minimal perturbations in transitional plane Couette flow. *Phys. Rev.* E **82** (2), 026316.

FALKOVICH, G. & VLADIMIROVA, N. 2018 Turbulence appearance and nonappearance in thin fluid layers. *Phys. Rev. Lett.* **121** (16), 164501.

GROSSMANN, S. 2000 The onset of shear flow turbulence. *Rev. Mod. Phys.* **72** (2), 603–618.

HAGAN, J. & PRIEDE, J. 2013 Weakly nonlinear stability analysis of magnetohydrodynamic channel flow using an efficient numerical approach. *Phys. Fluids* **25**, 124108.

HUSSAM, W.K., THOMPSON, M.C. & SHEARD, G.J. 2012 Optimal transient disturbances behind a circular cylinder in a quasi-two-dimensional magnetohydodynamic duct flow. *Phys. Fluids* **24**, 024105.

ITANO, T. & TOH, S. 2001 The dynamics of bursting process in wall turbulence. *J. Phys. Soc. Japan* **70** (3), 703–716.

JIMÉNEZ, J. 1990 Transition to turbulence in two-dimensional Poiseuille flow. *J. Fluid Mech.* **218**, 265–297.

KARNIADAKIS, G.E., ISRAELI, M. & ORSZAG, S.A. 1991 High-order splitting methods for the incompressible Navier–Stokes equations. *J. Comput. Phys.* **97** (2), 414–443.

KHAPKO, T., DUGUET, Y., KREILOS, T., SCHLATTER, P., ECKHARDT, B. & HENNINGSON, D.S. 2014 Complexity of localised coherent structures in a boundary-layer flow. *Eur. Phys. J.* E **37** (4), 1–12.

LEMOULT, G., SHI, L., AVILA, K., JALIKOP, S., AVILA, M. & HOF, B. 2016 Directed percolation phase transition to sustained turbulence in Couette flow. *Nat. Phys.* **12**, 254–258.

LINDBORG, E. 1999 Can the atmospheric kinetic energy spectrum be explained by two-dimensional turbulence? *J. Fluid Mech.* **388**, 259–288.

MELLIBOVSKY, F. & MESEGUER, A. 2015 A mechanism for streamwise localisation of nonlinear waves in shear flows. *J. Fluid Mech.* **779**, R1.

MOFFATT, H.K. 1967 On the suppression of turbulence by a uniform magnetic field. *J. Fluid Mech.* **28** (3), 571–592.

MOXEY, D. & BARKLEY, D. 2010 Distinct large-scale turbulent-laminar states in transitional pipe flow. *Proc. Natl Acad. Sci. USA* **107** (18), 8091–8096.

MÜLLER, U. & BÜHLER, L. 2001 *Magnetofluiddynamics in Channels and Containers*. Springer.

PARET, J., MARTEAU, D., PAIREAU, O. & TABELING, P. 1997 Are flows electromagnetically forced in thin stratified layers two dimensional? *Phys. Fluids* **9** (10), 3102–3104.

PEDLOSKY, J. 1987 *Geophysical Fluid Dynamics*. Springer.

POTHÉRAT, A. 2012 Three-dimensionality in quasi-two-dimensional flows: recirculations and Barrel effects. *Europhys. Lett.* **98** (6), 64003.

POTHÉRAT, A. & KLEIN, R. 2014 Why, how and when MHD turbulence at low *Rm* becomes three-dimensional. *J. Fluid Mech.* **761**, 168–205.

PRINGLE, C.C.T., WILLIS, A.P. & KERSWELL, R.R. 2012 Minimal seeds for shear flow turbulence: using nonlinear transient growth to touch the edge of chaos. *J. Fluid Mech.* **702**, 415–443.

REDDY, S.C., SCHMID, P.J., BAGGETT, J.S. & HENNINGSON, D.S. 1998 On stability of streamwise streaks and transition thresholds in plane channel flows. *J. Fluid Mech.* **365**, 269–303.

REYNOLDS, O. 1883 An experimental investigation of the circumstances which determine whether the motion of water shall be direct or sinuous, and of the law of resistance in parallel channels. *Phil. Trans. R. Soc. Lond.* **174**, 935–982.

SANSÓN, L.Z. & VAN HEIJST, G.J.F. 2000 Nonlinear Ekman effects in rotating barotropic flows. *J. Fluid Mech.* **412**, 75–91.

SAPARDI, A.M., HUSSAM, W.K., POTHÉRAT, A. & SHEARD, G.J. 2017 Linear stability of confined flow around a 180-degree sharp bend. *J. Fluid Mech.* **822**, 813–847.

SCHMID, P.J. & HENNINGSON, D.S. 2001 *Stability and Transition in Shear Flows*. Springer.

SHATS, M., BYRNE, D. & XIA, H. 2010 Turbulence decay rate as a measure of flow dimensionality. *Phys. Rev. Lett.* **105** (26), 264501.

SKUFCA, J.D., YORKE, J.A. & ECKHARDT, B. 2006 Edge of chaos in a parallel shear flow. *Phys. Rev. Lett.* **96** (17), 174101.

SOMMERIA, J. & MOREAU, R. 1982 Why, how, and when, MHD turbulence becomes two-dimensional. *J. Fluid Mech.* **118**, 507–518.

TABELING, P. 2002 Two-dimensional turbulence: a physicist approach. *Phys. Rep.* **362**, 1–62.

TREFETHEN, L.N., TREFETHEN, A.E., REDDY, S.C. & DRISCOLL, T.A. 1993 Hydrodynamic stability without eigenvalues. *Science* **261** (5121), 578–584.

WANG, J., LI, Q. & WEINAN, E. 2015 Study of the instability of the Poiseuille flow using a thermodynamic formalism. *Proc. Natl Acad. Sci. USA* **112** (31), 9518–9523.

WYGNANSKI, I. & CHAMPAGNE, F.H. 1973 On transition in a pipe. Part 1. The origin of puffs and slugs and the flow of a turbulent slug. *J. Fluid Mech.* **59** (2), 281–335.

WYGNANSKI, I., SOKOLOV, M. & FRIEDMAN, D. 1975 On transition in a pipe. Part 2. The equilibrium puff. *J. Fluid Mech.* **69** (2), 283–304.

ZAMMERT, S. & ECKHARDT, B. 2019 Transition to turbulence when the Tollmien–Schlichting and bypass routes coexist. *J. Fluid Mech.* **880**, R2.